Absorption cross-section spectrum of single CdSe/ZnS nanocrystals revealed through photoluminescence excitation spectroscopy

AUTHOR(S):

Ihara, Toshiyuki; Kanemitsu, Yoshihiko

PHYSICAL REVIEW B **92**, 155311 (2015)

Absorption cross-section spectrum of single CdSe/ZnS nanocrystals revealed through photoluminescence excitation spectroscopy

Toshiyuki Ihara and Yoshihiko Kanemitsu
Institute for Chemical Research, Kyoto University, Uji, Kyoto 611-0011, Japan
(Received 28 May 2015; revised manuscript received 26 September 2015; published 19 October 2015)

The absorption spectrum represents an important aspect of single semiconductor nanocrystals (NCs), revealing the morphology and orientation of the NCs. By conducting quantitative photoluminescence excitation spectroscopy based on a single-photon counting method, we succeed in clarifying the absorption cross-section spectrum of neutral excitons in single CdSe/ZnS NCs. With the values of the absorption cross section, we reveal that the intensity saturation of the neutral-exciton emission can be explained by considering the Poisson statistics for incident photons and by the small quantum yield of the biexciton emission. We also evaluated quantitatively the biexciton emission contribution and the ionization rate of NCs that appear at increased incident photon fluxes.

DOI: 10.1103/PhysRevB.92.155311 PACS number(s): 78.67.−n, 42.50.Nn, 78.20.Ci, 78.55.Et

I. INTRODUCTION

Semiconductor nanocrystals (NCs) have been studied intensively for two decades, which has clarified our understanding of the fundamental physics associated with the quantum confinement effect [1]. Since they exhibit high emissivity, they can be used for applications of various photonic devices, such as light-emitting diodes and single-photon emitters [2,3]. The neutral excitons, formed with an electron in the conduction band and a hole in the valence band, are the most fundamental excited states in NCs. The optical transitions of neutral excitons—photoabsorption and photoemission—are characterized by several parameters, such as the absorption cross section (σ), the photoluminescence (PL) lifetime (τ), and the quantum yield (QY) [4–11]. The value of σ determines the ratio between the incident photon flux and the average exciton density [4–6], whereas the QY is defined as the ratio between τ and the radiative recombination lifetime [7–14]. Both σ and QY are crucial parameters for characterizing the NCs; thus, it is an important task to establish experimental methods for evaluating them. Concerning σ, however, there have been no experiments, to our knowledge, on single NCs that achieved its evaluation in a unit of absorption cross section for a wide spectral range. This is because NCs have σ values that are typically on the order of 10^{-14}–10^{-15} cm^2 [4–6], which is too small to be evaluated by measuring the optical transmittance [15–23]. The measurement of neutral-exciton emission QY on single NCs is also experimentally challenging [7,8]. Because of the difficulties associated with evaluating σ and QY, the unique properties of individual NCs—such as the nonlinear effect that appears at high incident photon fluxes—have been difficult to elucidate quantitatively.

One of the various approaches for revealing absorption processes in semiconductor nanostructures is PL excitation (PLE) spectroscopy, which can be obtained by measuring the PL intensity as a function of excitation photon energy. This method reveals the lineshape of the absorption spectrum with an impressive signal-to-noise ratio, even on single nanostructures [24–27]. However, one crucial problem associated with PLE measurements is that they usually do not provide the value of σ. This originates from the difficulties to evaluate the QY of the PL and to determine certain experimental conditions—such as the detection efficiency and incident photon flux. Recently, new aspects of single-NC photoemission have been studied using various methods based on single-photon counting methods, such as the measurements of second-order photon correlation and time-dependent fluctuations of PL spectrum and lifetime [6,10,14,28]. These studies have enabled us to estimate the QY of the biexcitons and the neutral excitons. This means that, by conducting quantitative PLE spectroscopy based on the single-photon counting method, one can measure the absorption spectrum of single CdSe/ZnS NCs. In this way, an experimental basis for measuring the absorption spectrum of single semiconductor NCs can be established.

In this paper, we quantitatively investigate the absorption cross-section spectrum and emission QY of neutral excitons in single CdSe/ZnS NCs using an experimental technique that combines PLE spectroscopy and the single-photon counting method. We determine the QY of neutral-exciton emission from the relationship between the fluctuating PL intensity and lifetime. The conversion from the PLE spectrum to the absorption cross-section spectrum is realized through evaluation of parameters such as the detection efficiency and incident photon flux. The quantitative values of QY and σ enable us to reveal that the PL of neutral excitons show an intensity saturation induced by Poisson statistics for the incident photons and by the small biexciton quantum yield. The biexciton emission contribution and the ionization rate of NCs at increased incident photon fluxes are also studied quantitatively.

II. EXPERIMENT

For the conversion from PL intensity to σ, the following equation is used:

$$\sigma(h\nu) = I/(F \cdot \xi \cdot \eta_X \cdot j_{exc}), \tag{1}$$

where $h\nu$ is photon energy, I is the detected photon count rate (s^{-1}), F is the repetition rate of the excitation pulse (s^{-1}), ξ is the detection efficiency, η_X is the QY of the neutral exciton emission, and j_{exc} is the excitation photon flux (photons/cm^2). This equation is obtained from the following two equations related to the average exciton density $\langle N \rangle$:

$$\langle N \rangle = \sigma(h\nu) \cdot j_{exc}(h\nu), \tag{2}$$

$$I = F \cdot \xi \cdot \eta_X \cdot \langle N \rangle. \tag{3}$$

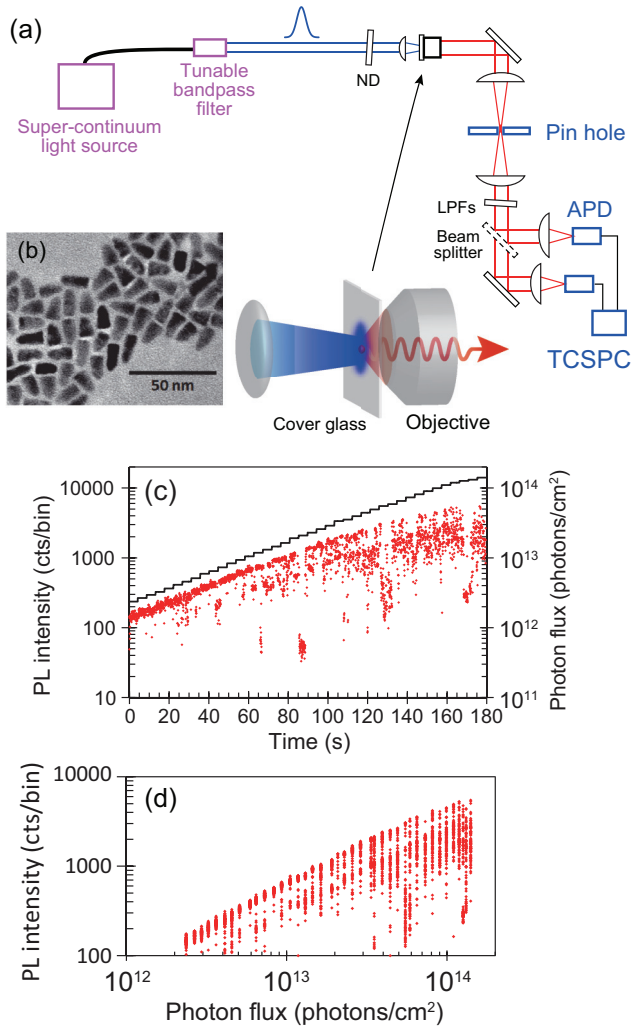

FIG. 1. (Color online) (a) A schematic diagram of the measurement setup for the quantitative PL excitation spectroscopy. The PL is detected by a set of an APD and a time-correlated single-photon counting (TCSPC) board. (b) A TEM image of the sample. (c) PL intensity of a single CdSe/ZnS NC (red dots) measured at various values of j_{exc} (black line). (d) PL intensity plotted as a function of j_{exc}.

Equation (2) defines the value of σ. Equation (3) describes the relation between I and $\langle N \rangle$, which is available for single-photon emission under the linear regime, where $\langle N \rangle \ll 1$. The amount of excitons in a NC can be counted as a whole number because of the quantum confinement effect [1].

In order to experimentally evaluate these parameters, we developed the measurement system shown in Fig. 1(a). Monochromatic light obtained from a supercontinuum light source (SC-400PP, Fianium) operating at a repetition rate of 5 MHz was used as an excitation source. The bandwidth of the excitation light was set at 8 nm by using a tunable bandpass filter (Super Chrome; Fianium). The samples of single CdSe/ZnS NCs (Qdot655; Life Technologies), which were prepared by spin coating on cover glass with a film of polymethylmethacrylate, were illuminated by the excitation light through an achromatic lens with a focal length of 2.5 cm. Figure 1(b) shows a transmission electron microscope (TEM) image of the sample. The total sizes of the CdSe/ZnS NCs are $14 \times 7 \times 7\,\mathrm{nm}^3$. Because the Qdot655 have nonspherical morphologies, the value of σ depends on the orientation of the particles. The PL from the NCs was collected by a 100× oil-immersion objective lens with numerical aperture (N.A.) of 1.3 (N100×-PFO; Nikon). The experiments were performed at room temperature.

The PL from a single NC was selectively extracted by a pinhole with a diameter of 0.4 mm, which corresponds to a detection area of $12.6\,\mu\mathrm{m}^2$. The PL from a single NC was filtered by long-pass filters (LPFs), and then detected by a set of avalanche photodiodes (APDs) placed under Hanbury Brown-Twiss geometry. These APDs were used to measure the PL lifetime and second-order photon correlation simultaneously. We measured the excitation power at the position between the pinhole and the LPFs, and evaluated j_{exc} by assuming that the excitation area is $12.6\,\mu\mathrm{m}^2$. For PLE measurements, the excitation power densities were kept at almost the same value for various excitation wavelength by using variable neutral density (ND) filters. We measured the optical transmittance from the position after the objective lens to the position before the APDs for 655 nm, and determined it to be 0.26. We estimated the coupling efficiency between the polarized PL and the objective (with an N.A. of 1.3) to be 0.3 ± 0.1 [7]. The APD has a detection efficiency of 0.35 at 655 nm. From these values, we determined ξ to be 0.03 ± 0.01.

III. RESULTS AND DISCUSSION

Figure 1(c) shows the PL intensities measured at various values of j_{exc} from 2.4×10^{12} to 1.4×10^{14} photons/cm^2. The wavelength of the excitation light (λ_{exc}) was set at 520 nm. For each value of j_{exc}, which is shown by the solid black line, the PL was integrated for 4 s with 0.5 s intervals. The PL intensities, shown as red dots, are plotted with units of counts (cts) per binning time (bin), where we set the bin time at 50 ms. In Fig. 1(d), we plot the PL intensity as a function of j_{exc}. For $j_{exc} = 2.4 \times 10^{12}$ photons/cm^2, the PL is dominated by a signal with an intensity of 150 cts/bin. This contribution shows a linear increase with j_{exc} and dominates the PL signal for the weak excitation regime below 2×10^{13} photons/cm^2 (i.e., <85 s). These signals, showing the highest PL intensities, are attributed to emissions from neutral excitons [11–13]. For values of j_{exc} above 2×10^{13} photons/cm^2, the appearance of additional contributions with smaller intensities increases. These signals are attributed to the emission of so-called intermediate states, such as charged excitons, doubly charged excitons, and dark states associated with surface trap states [11–13]. To reveal the characteristics of neutral exciton emissions, the incident photon flux should be adjusted to minimize the appearance of these intermediate states.

Next, we show PL data of the same NC, integrated for 200 s at $j_{exc} = 1.3 \times 10^{13}$ photons/cm^2. Figure 2(a) shows time-dependent PL intensities plotted for 120–160 s. The right panel shows a histogram of occurrences integrated for 200 s. Figure 2(b) shows the corresponding PL lifetimes obtained by applying a single exponential fitting to the PL decay curves for each bin time, as we have reported in a previous paper [28]. Figure 2(c) shows the relationship between PL lifetime and intensity, which is known as the fluorescence

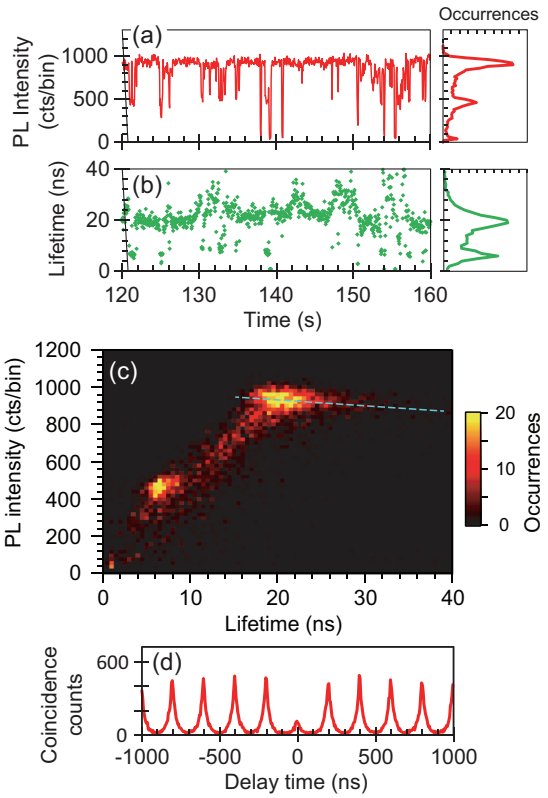

FIG. 2. (Color online) (a) A time trace of PL intensities measured at a fixed value of j_{exc} plotted for 120–160 s (left panel) and their occurrences integrated for 200 s (right panel). (b) A time trace of PL lifetimes plotted for 120–160 s (left panel) and the occurrence plot (right panel). (c) Results of FLID analysis. (d) Results of the second-order photon correlation analysis.

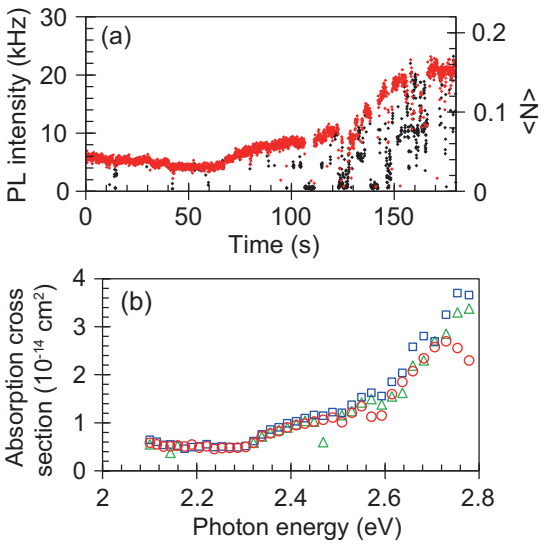

FIG. 3. (Color online) (a) PL intensity of a single CdSe/ZnS NC measured at various values of λ_{exc}. (b) Absorption cross-section spectrum obtained by quantitative PL excitation spectroscopy. The measurements were conducted three times, which are plotted as circles, squares, and triangles.

lifetime-intensity distribution (FLID) map. Figure 2(d) shows the second-order photon correlation, obtained from the same set of data. The data were analyzed only for the neutral exciton contributions by selecting the signals with PL intensities larger than 800 cts/bin. In the FLID map, neutral exciton contributions appear above 800 cts/bin with lifetime at 20 ns. Charged-exciton contributions appear at small PL intensities (500 cts/bin) with lifetimes of 6.5 ns.

The contributions with long lifetimes (i.e., >30 ns) are attributed to neutral excitons modified by quantum-confined Stark effect (QCSE), whose radiative recombination lifetimes increase because of the decrease in the overlap between electrons and holes [28]. As indicated by the blue dotted line, the QCSE-modified neutral excitons show a slight decrease in PL intensity for longer lifetimes. Since the QCSE changes the radiative recombination lifetime, while it does not result in a significant change of nonradiative recombination rate (k_{NR}), the value of k_{NR} can be determined by comparing the experimental data with the following equation: $\eta_X = 1 - (k_{NR} \cdot \tau)$. From the slope of the blue line, we determine that $k_{NR} = 5\,\mu s^{-1}$. Thus, for the main contribution of neutral excitons at 20 ns, η_X can be estimated as 0.9.

Figure 3(a) shows the PL intensity measured as a function of λ_{exc}, where λ_{exc} ranges from 590 to 434 nm with a step size of 4 nm. The excitation photon energies (2.1–2.86 eV) are much smaller than the bandgap energy of the ZnS shell (3.7 eV). This means that the optical excitation usually results in creations of carriers inside the CdSe core. The excited carriers relax to the ground states in the core and emit photons with QY of near unity. This means that the effects of nonradiative recombination processes associated with trap states inside and outside the NCs are negligible, and thus, it enables us to consider that the relaxation process of excited carriers does not depend on the excitation photon energy. For each value of λ_{exc}, the data were integrated for 4 s with 0.5 s intervals. We selectively plot the neutral-exciton contribution with red dots, assuming that the signals with lifetimes from 15 to 30 ns correspond to neutral exciton contributions. Other contributions of intermediate states are plotted with black dots. On the right side of the y axis, the value of $\langle N \rangle$ is also presented, which was determined using Eq. (3). The results confirm that the PL was measured for $\langle N \rangle < 0.16$, which means that the $\langle N \rangle \ll 1$ condition was satisfied for this measurement. Since $\xi \cdot \eta_X \cdot \langle N \rangle < 0.005$, the detection count rate is less than 0.5% of trigger frequency. This enables us to consider that the effect of counting loss is negligible.

Figure 3(b) shows the result of the absorption cross-section spectrum of neutral excitons, obtained by averaging the neutral exciton contributions shown in Fig. 3(a). The values of σ were evaluated from PL intensities by converting them via Eq. (1). For the purpose of reproducibility, we conducted the measurements three times, as plotted by circles, squares, and triangles. The values of σ ranged from 5×10^{-15} at 2.1 eV to 3×10^{-14} cm^2 at 2.7 eV. The data show a gradual increase of σ for higher energies, including an onset structure at around 2.3–2.5 eV. These characteristics of the absorption spectrum were also observed by using transmission spectroscopy. The absence of sharp structures in the excited states for the CdSe/ZnS NCs with large sizes of $14 \times 7 \times 7$ nm^3 is consistent

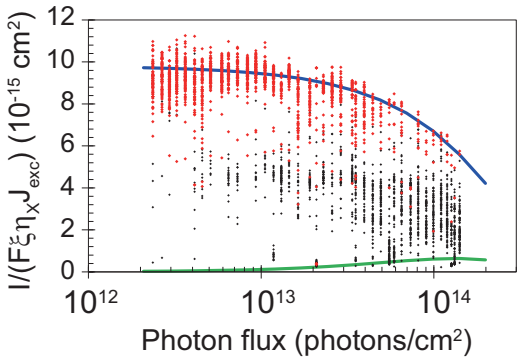

FIG. 4. (Color online) Results of $I/F \cdot \xi \cdot \eta_X \cdot j_{exc}$ plotted as a function of j_{exc}. The neutral exciton contribution is plotted with red dots, whereas the contributions of other intermediate states are plotted with black dots. The green line corresponds to the contribution of biexciton emission, whereas the blue line corresponds to the sum of neutral exciton emission and biexciton emission.

with earlier works [4], since they reported similar transmission spectra without sharp peaks. The order of σ, which ranged from 5×10^{-15} to 3×10^{-14}, also agrees with values reported by them. From these results, we conclude that the quantitative PLE spectroscopy based on the single-photon counting method enables us to reveal absorption cross-section spectrum of neutral excitons in single CdSe/ZnS NCs.

When σ of a single NC is determined, the value of $\langle N \rangle$ can be also evaluated from j_{exc} through Eq. (2), which enables us to study quantitatively the nonlinearity in the PL characteristics appearing at high values of j_{exc}. In this context, the mechanism for the appearance of the PL nonlinearities, such as PL intensity saturation and appearance of intermediate states, as we have presented in Fig. 1(c), can be quantitatively studied. Finally, we discuss the nonlinearity of the PL intensity by showing a comparison between the experimental results and calculated results. Because we have determined the values of ξ, η_X, and j_{exc}, we can plot $I/F \cdot \xi \cdot \eta_X \cdot j_{exc}$, which corresponds to σ for the weak excitation limit. Figure 4 shows the j_{exc} dependence of $I/F \cdot \xi \cdot \eta_X \cdot j_{exc}$ for neutral exciton emission (red dots) and for other contributions of intermediate states (black dots). The blue line corresponds to the result of calculations for $I_X + I_{XX}$, where I_X is the neutral exciton contribution and I_{XX} is the biexciton emission contribution. We consider that the effect of the peak shift due to Coulomb interactions in biexciton excited states is negligible, since the absorption structure is broader than the order of Coulomb shift. According to previous works [6,10,14], the excitation probability of single NCs can be written by the Poisson distribution. By using this, the contributions of neutral excitons and biexcitons can be written as the following equations:

$$I_X = F \cdot \xi \cdot \eta_X \cdot (\langle N \rangle + \langle N \rangle^2/2 + \langle N \rangle^3/6) \cdot \exp(-\langle N \rangle), \quad (4)$$

$$I_{XX} = F \cdot \xi \cdot \eta_{XX} \cdot (\langle N \rangle^2/2 + \langle N \rangle^3/6) \cdot \exp(-\langle N \rangle), \quad (5)$$

where η_{XX} is the QY of biexciton emission. From the ratio between the center peak and side peaks of the second-order photon correlation shown in Fig. 2(d), we determine that $\eta_{XX} = 0.23$ [6,10,14]. The green line corresponds to I_{XX}. The calculated result of $I_X + I_{XX}$, which shows a saturation curve for large values of j_{exc}, agrees with the experimental results. This agreement means that the PL of neutral excitons shows an intensity saturation governed by Poisson distribution.

When we adopted the above method on several single NCs, we found that the values of QY and σ depend on the particles in question. The values of QY ranged from 0.7 to 0.9, whereas the values of σ at 520 nm ranged from 5×10^{-15} to 14×10^{-15} cm^2. The appearances of the range of values are consistent with our expectations; because the current samples of Qdot655 have nonspherical morphologies [29], the values of σ depend on the orientation of the particles. This ability to obtain QY and σ for individual NCs is an important advantage of single-particle absorption spectroscopy, which enables us to reveal morphology-dependent optical absorption properties.

In addition, the particle-dependent nonlinearity—i.e., the appearance of charged excitons (X^-) and doubly charged excitons—could also be revealed by using our method. The appearance of X^- at high excitation power indicates that the occurrence of PL blinking strongly depends on the incident photon flux. This feature can be explained by a model considering the Auger-assisted ionization process, as discussed in earlier works [13,30]. By using the determined value of σ, we estimate that the transition from the neutral-exciton-dominated regime to the charged-exciton-dominated regime occurs at $\langle N \rangle_{X \to X^-} \cong 0.3$. By measuring $\langle N \rangle_{X \to X^-}$ on certain NCs, we observed different values, which depended on the particles in question. We believe that the value of the transition, $\langle N \rangle_{X \to X^-}$, and also the estimated contributions of biexciton emission, might be helpful in understanding the detailed mechanism of the Auger-assisted ionization process [13,30–32].

IV. CONCLUSION

In summary, we showed that the emission QY and the absorption cross-section spectrum of neutral excitons in single CdSe/ZnS NCs can be revealed by measurements of fluctuating PL intensity and lifetime, second-order photon correlation, and the quantitatively determined values of detection efficiency and excitation photon flux. We showed that the obtained QY and σ values of neutral excitons are consistent with the incident-photon-flux-dependent PL intensities, showing a saturation curve governed by Poisson distributions. The current technique of quantitative PLE spectroscopy can be applied to smaller molecules with values of σ that are less than 10^{-14} cm^2, which are difficult to measure with conventional methods based on optical transmittance measurements. Thus, this paper establishes an experimental basis for a deep understanding of the crucial roles of the morphologies, charging, QCSE, and orientation on the optical properties of nano-objects. This can be extended to various nanostructures such as NCs with unique morphologies (e.g., CdSe/CdS core-shell particles), quantum heterostructures, and carbon nanotubes.

ACKNOWLEDGMENT

Part of this paper was supported by JSPS KAKENHI Grant No. 25247052 and JST-CREST.

[1] V. I. Klimov, Annu. Rev. Condens. Matter Phys. **5**, 285 (2014).
[2] Y. Shirasaki, G. J. Supran, M. G. Bawendi, and V. Bulović, Nat. Photon. **7**, 13 (2013).
[3] M. J. Fernée, P. Tamarat, and B. Lounis, Chem. Soc. Rev. **43**, 1311 (2014).
[4] C. A. Leatherdale, W.-K. Woo, F. V. Mikulec, and M. G. Bawendi, J. Phys. Chem. B **106**, 7619 (2002).
[5] J. Nanda, S. A. Ivanov, H. Htoon, I. Bezel, A. Piryatinski, S. Tretiak, and V. I. Klimov, J. Appl. Phys. **99**, 034309 (2006).
[6] Y.-S. Park, A. V. Malko, J. Vela, Y. Chen, Y. Ghosh, F. García-Santamaría, J. A. Hollingsworth, V. I. Klimov, and H. Htoon, Phys. Rev. Lett. **106**, 187401 (2011).
[7] X. Brokmann, L. Coolen, M. Dahan, and J. P Hermier, Phys. Rev. Lett. **93**, 107403 (2004).
[8] B. R. Fisher, H.-J. Eisler, N. E. Stott, and M. G. Bawendi, J. Phys. Chem. B **108**, 143 (2004).
[9] M. Grabolle, M. Spieles, V. Lesnyak, N. Gaponik, A. Eychmüller, and U. Resch-Genger, Anal. Chem. **81**, 6285 (2009).
[10] G. Nair, J. Zhao, and M. G. Bawendi, Nano Lett. **11**, 1136 (2011).
[11] P. Spinicelli, S. Buil, X. Quélin, B. Mahler, B. Dubertret, and J.-P. Hermier, Phys. Rev. Lett. **102**, 136801 (2009).
[12] C. Galland, Y. Ghosh, A. Steinbrück, M. Sykora, J. A. Hollingsworth, V. I. Klimov, and H. Htoon, Nature **479**, 203 (2011).
[13] C. Galland, Y. Ghosh, A. Steinbrück, J. A. Hollingsworth, H. Htoon, and V. I. Klimov, Nat. Commun. **3**, 908 (2012).
[14] M. Manceau, S. Vezzoli, Q. Glorieux, F. Pisanello, E. Giacobino, L. Carbone, M. De Vittorio, and A. Bramati, Phys. Rev. B **90**, 035311 (2014).
[15] S. Berciaud, L. Cognet, and B. Lounis, Phys. Rev. Lett. **101**, 077402 (2008).
[16] A. Gaiduk, M. Yorulmaz, P. V. Ruijgrok, and M. Orrit, Science **330**, 353 (2010).
[17] M. Celebrano, P. Kukura, A. Renn, and V. Sandoghdar, Nat. Photon. **5**, 95 (2011).
[18] J. Giblin, F. Vietmeyer, M. P. McDonald, and M. Kuno, Nano Lett. **11**, 3307 (2011).
[19] J.-C. Blancon, M. Paillet, H. N. Tran, X. T. Than, S. A. Guebrou, A. Ayari, A. S. Miguel, N.-M. Phan, A.-A. Zahab, J.-L. Sauvajol, N. D. Fatti, and F. Vallee, Nat. Commun. **4**, 3542 (2013).
[20] A. Crut, P. Maioli, N. D. Fatti, and F. Vallee, Chem. Soc. Rev. **43**, 3921 (2014).
[21] A. Högele, S. Seidl, M. Kroner, K. Karrai, R. J. Warburton, B. D. Gerardot, and P. M. Petroff, Phys. Rev. Lett. **93**, 217401 (2004).
[22] P. Kukura, M. Celebrano, A. Renn, and V. Sandoghdar, Nano Letters **9**, 926 (2009).
[23] P. Kukura, M. Celebrano, A. Renn, and V. Sandoghdar, J. Phys. Chem. Lett. **1**, 3323 (2010).
[24] H. Htoon, P. J. Cox, and V. I. Klimov, Phys. Rev. Lett. **93**, 187402 (2004).
[25] T. Ihara, Y. Hayamizu, M. Yoshita, H. Akiyama, L. N. Pfeiffer, and K. W. West, Phys. Rev. Lett. **99**, 126803 (2007).
[26] T. Ihara, S. Maruyama, M. Yoshita, H. Akiyama, L. N. Pfeiffer, and K. W. West, Phys. Rev. B **80**, 033307 (2009).
[27] N. J. Borys, M. J. Walter, J. Huang, D. V. Talapin, and J. M. Lupton, Science **330**, 1371 (2010).
[28] T. Ihara and Y. Kanemitsu, Phys. Rev. B **90**, 195302 (2014).
[29] F. Masia, N. Accanto, W. Langbein, and P. Borri, Phys. Rev. Lett. **108**, 087401 (2012).
[30] N. Yoshikawa, H. Hirori, H. Watanabe, T. Aoki, T. Ihara, R. Kusuda, C. Wolpert, T. K. Fujiwara, A. Kusumi, Y. Kanemitsu, and K. Tanaka, Phys. Rev. B **88**, 155440 (2013).
[31] B. Fisher, J. M. Caruge, D. Zehnder, and M. Bawendi, Phys. Rev. Lett. **94**, 087403 (2005).
[32] R. M. Kraus, P. G. Lagoudakis, J. Muller, A. L. Rogach, J. M. Lupton, J. Feldmann, D. V. Talapin, and H. Weller, J. Phys. Chem. B **109**, 18214 (2005).